https://doi.org/10.15407/ujpe71.4.359

YU. SKRYSHEVSKI,[1] A. VAKHNIN,[1] YU. PIRYATINSKI,[1] SHAIMA M. ABD AL-BAQI,[2] H. SITTER,[2] A. KADASHCHUK [1,3]

[1] Institute of Physics, Nat. Acad. of Sci. of Ukraine
*(46, Prosp. Nauky, Kyiv 03028, Ukraine; e-mail: kadash@iop.kiev.ua)*
[2] Institute of Semiconductor and Solid State Physics, Johannes Kepler University of Linz
*(A-4040 Linz, Austria)*
[3] Soft Matter Optoelectronics and Bavarian Polymer Institute (BPI), University of Bayreuth
*(30, Universitäts Str., 95448 Bayreuth, Germany; e-mail: kadash@iop.kiev.ua)*

# MORPHOLOGY-DEPENDENT DEFECT STATES IN RUBRENE CRYSTALLINE FILMS GROWN BY HOT-WALL EPITAXY

*Rubrene nanostructures grown on mica substrates by Hot-Wall Epitaxy were investigated using photoluminescence (PL) and thermally stimulated luminescence (TSL) spectroscopy. Different film morphologies, characterized by optical and electron microscopy, were obtained by varying the deposition conditions. Temperature-dependent PL spectra are found to depend substantially on the morphology of the rubrene layers. Films grown with short deposition times exhibit PL spectra dominated by intrinsic exciton emission, with only weak quenching with increasing temperature. In contrast, films grown at longer deposition times and higher substrate temperatures display additional emissive species, and their PL intensity shows a strong temperature quenching. The main results of this study are as follows: (i) A specific structure-related defect state is created in rubrene films grown at extended deposition times and elevated substrate temperatures, acting as a distinct hole trap with the depth $E_t$ = 0.23 eV, as measured by TSL. This defect gives rise to a broad, low-energy emission band that dominates the room-temperature PL spectra; (ii) deliberate oxidation of rubrene crystals demonstrates that the hole trap observed in TSL is not oxygen-related but originates from an intrinsic crystalline defect; (iii) TSL reveals a continuous distribution of shallow localized states, reminiscent of band-tail states, arising from intrinsic energetic disorder in the material. These shallow states are responsible for the very low temperature TSL features near 30 K and for the red shift of the PL spectra with increasing delay time observed in time-resolved PL measurements.*

*Keywords*: rubrene, hot-wall epitaxy, nanostructures, defect state, film morphology, energetic disorder, thermally stimulated luminescence.

## 1. Introduction

Organic semiconducting materials are of increasing technological and fundamental interest due to remarkable technological breakthroughs made by molecular electronics in the last decade. Rubrene is a very attractive organic semiconductor possessing many promising properties which make it a material of choice for the fabrication of single crystal organic field effect transistors (OFETs). It shows the highest reported charge carrier mobility in single-crystal OFET (~20 cm$^2$/Vs) [1–3]. On the other hand, the fabrication of rubrene thin films has turned out to be a difficult task. In spite of considerable efforts made to fabricate OFETs based on rubrene thin films [4–6], the largest mobility obtained so far in these devices is 2.5 cm$^2$/Vs [6], which is still much less than that in single-crystalline bulk material. The main difference between bulk and thin film material is the degree of crystallinity. Consequently, the main effort has been directed toward improving the crystallographic order

---

Citation: Skryshevski Yu., Vakhnin A., Piryatinski Yu., Al-Baqi S.M.A., Sitter H., Kadashchuk A. Morphology-dependent defect states in rubrene crystalline films grown by hot-wall epitaxy. *Ukr. J. Phys.* **71**, No. 4, 359 (2026). https://doi.org/10.15407/ujpe71.4.359.

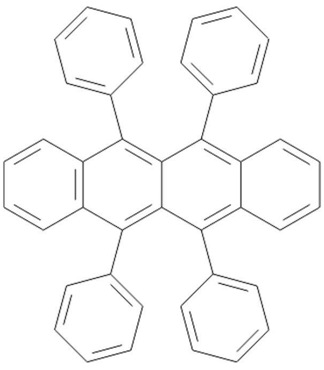

Scheme 1

in rubrene layers. Since there is no lattice matched substrate available, the only chance to approach the goal of highly ordered structures is to use an optimized growth regime. Due to the weak Van der Waals type coupling between molecules, a deposition process as close as possible to thermodynamic equilibrium may be appropriate. The local dynamic equilibrium at the growing surface allows a multiple impingement and re-evaporation of the molecules. Supported by an enhanced surface mobility, the rubrene molecules can find the optimum position on the substrate to form a highly ordered structure, which can lead to a layer of enhanced crystallinity. The method of choice to provide such growth conditions is the Hot Wall Epitaxy (HWE) [7–9].

It is generally accepted that charge-carrier traps in organic semiconducting materials are critical to device performance. The presence of relatively deep localized charge-carrier states can severely degrade the device performance since trap states reduce the carrier mobility, disturb the field distribution and affect the driving voltage in certain types of organic optoelectronic devices. Direct information about the nature and the identity of trap states is therefore crucial for the fabrication of advanced organic optoelectronic devices. In organic materials the film morphology plays a fundamental role in charge carrier transport. Currently there exists evidence that charge carrier trapping is a key issue in this context, but the exact relations remain unclear. Therefore, it is important to elucidate the possible origin of the defect states in thin HWE-grown rubrene films as well. In this paper, we present a temperature-dependent steady-state- and time-resolved photoluminescence (PL) investigation of rubrene films grown by HWE, as well as a study of charge-carrier trapping in these films by thermally-stimulated luminescence (TSL).

## 2. Experimental

The rubrene (see Scheme 1) source material was purchased from Aldrich (purity $> 98\%$) and purified by threefold sublimation under dynamic vacuum at $10^{-5}$ mbar. The rubrene layers were evaporated in a standard HWE reactor [9] on freshly cleaved $2M_1$ muscovite mica using a source temperature ($T_s$) of 235 °C for the evaporation of rubrene. The surface mobility of the rubrene molecules was influenced by the substrate temperature ($T_{\rm sub}$) in the range from 90 °C to 120 °C. The surface morphology of the rubrene layers was investigated by optical and scanning electron microscopy (SEM).

The conventional steady-state PL (continuous wave (cw-PL)) was measured at temperatures ranging from 4.2 K to 300 K using an optical helium cryostat. All PL spectra were corrected for background radiation and instrumental spectral response. Time-resolved PL measurements were performed with a monochromator (linear dispersion 0.8 nm/mm) and a 0.1 ns gating registration system containing a photomultiplier tube and a stroboscopic oscilloscope. A nitrogen laser with a pulse duration of 8 ns and a repetition rate of 100 Hz was used for optical excitation at 337.1 nm. PL emission was detected during the laser excitation pulse either at the leading edge of the laser excitation pulse (starting from ∼0.8 ns after the pulse onset), or at the tailing edge of the laser pulse after a variable delay times ($t_{\rm del}$ ) with respect to the onset of the laser pulse. For the experimental details, see, for instance, Ref. [10]. The rubrene films did not exhibit any notable photo-degradation during the measurements.

Thermally stimulated luminescence (TSL) is the phenomenon of luminescent emission after removal of excitation under conditions of increasing temperature. Generally, in the TSL method the trapping states are first populated by photogeneration of charge carriers, usually at low temperatures in order to prevent a fast escape. The trapped charge carriers are released by heating up the sample with a linear temperature ramp, while the luminescence due to radiative recombination is recorded as a function of temperature. If an energy distribution of the trap states exists, TSL spectra represent a complicated convolution of contributions from different traps at different energies and the fractional heating technique has to be applied. This technique is based on cycling the sample with a large number of small temperature oscillations superimposed on a constant heating run [11, 12]. Thus, TSL is a useful tool for determining the trap depths even when traps are not well separated in energy, or are continuously distributed, and it also allows an analysis of the trap spectra even when they are complex. Unfortunately, the interpretation of TSL phenomena in amorphous organic materials with hopping charge transport is not so straightforward as in inorganic crystalline materials due to the presence of strongly localized energetically disordered states forming a Gaussian density-of-states (DOS) distribution and the lack of the band edge. Therefore, it is not obvious which sites play a role as traps, and which are regular transport states. Therefore, a hopping model of TSL in disordered organic materials has been suggested in Refs. [13, 14], which describes most of the basic features of the TSL in disordered organic materials and permits the calculation of the DOS distribution from the TSL data.

TSL measurements were carried out using a home-built setup operable from 4.2 to 350 K using a temperature-controlled helium cryostat. After cooling down to 4.2 K, the samples were photo-excited, usually for 1 min, by a high-pressure 500 W mercury lamp with an appropriate set of optical filters for light selection. After the photoexcitation, the TSL was detected in a photon-counting mode with a cooled photomultiplier, positioned next to the cryostat window. The TSL measurements were performed either at a constant heating rate of $\beta = 0.15$ K/s or in the fractional heating regime. The details of the used TSL method were described previously in Refs. [11–13].

## 3. Results

### *3.1. Rubrene film morphologies*

Two different growth regimes were used to fabricate the rubrene layers by HWE. In the first set, a low growth temperature of 90 °C and a short deposition time of 15 min was used, whereas in the other case a higher growth temperature of 120 °C and a longer deposition time of 3 hours was used. Typical micrographs and SEM pictures of the obtained morphologies are shown in Fig. 1. The top row shows the optical micrographs, while the bottom row shows the SEM micrographs for the two growth regimes.

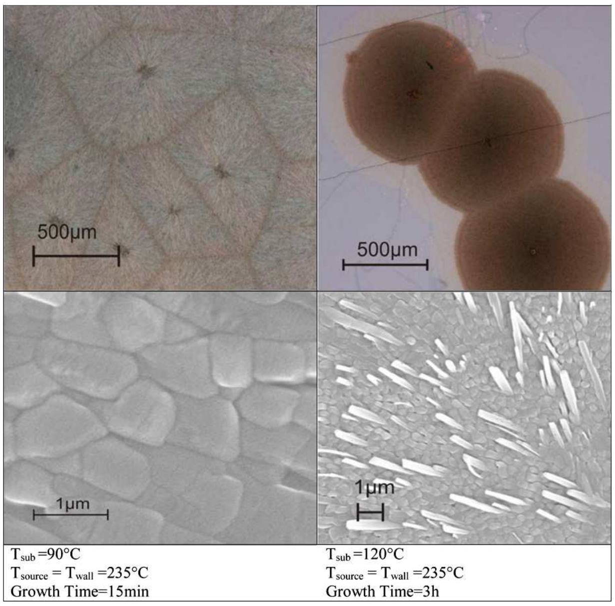

***Fig. 1.*** Optical (top row) and SEM pictures (lower row) of rubrene thin films grown by HWE on mica (001) substrates. The samples were grown at 90 °C for 15 min (left column) and at 120 °C for 3 hours (right column)

At low growth temperatures and short deposition time the whole substrate surface was covered with spherulite structures intersecting each other. The zoom in by SEM showed small crystallites with a diameter of 0.5–1 $\mu$m with a preferential alignment along the radial direction of the spherulites. A first onset of an inner structure could be observed in the center of the spherulites (dark spots in the optical micrographs, Fig. 1); however the main part of the rubrene layers was dominated by the crystalline islands (grains). This type of samples is hereafter called *“islands”* structures.

In the case of higher substrate temperatures and longer deposition time the surface mobility of the rubrene molecules was enhanced, resulting in an incomplete coverage of the mica substrates as clearly seen in the optical microscope. The spherulites consisted of a dominating inner part surrounded by an outer ring, which showed essentially the same structure as the low temperature samples. However, the inner part was dominated by the formation of whisker-like structures as clearly revealed in the SEM pictures. On top of the islands formed in the early stage

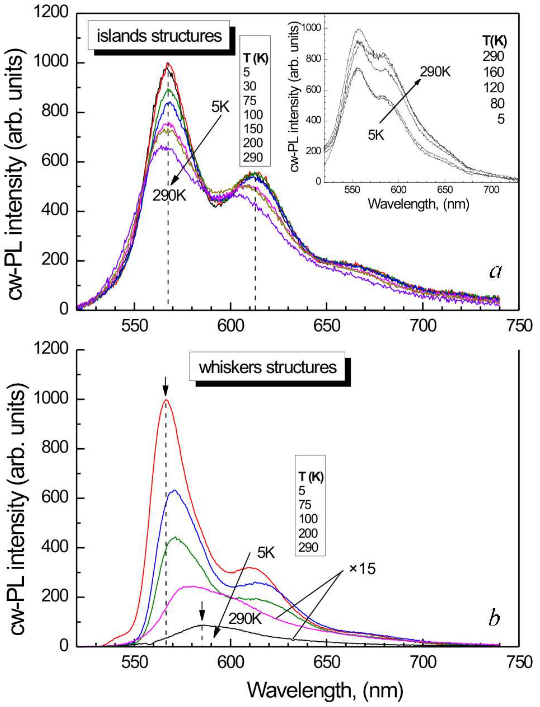

***Fig. 2.*** cw-PL spectra of the selected HWE-grown rubrene films: "islands" structures (*a*) and "whiskers" structures (*b*) measured at different temperatures. Inset: cw-PL spectra of rubrene dispersed in a polystyrene host film

of growth additional columnar structures were formed following the main radial direction of the spherulites and clearly protruding from the layer, therefore this type of samples is called "*whiskers*" structures in the following description.

### *3.2. Photoluminescence study*

We found that the PL properties of rubrene films grown by HWE on a mica substrate depend substantially on the layer's morphology governed by the film deposition temperature and growth time. Temperature-dependent cw-PL spectra of two representative examples of rubrene films featuring "*islands*" and "*whiskers*" structures (cf. Fig. 1) are depicted in Fig. 2, *a* and 2, *b*, respectively. PL spectra were measured at different temperatures in the range from 5 K to 290 K. The *low-temperature* ($T = 5$ K) PL spectra of both samples are virtually similar to those observed before in bulk rubrene single crystals [15] and exhibit a characteristic fine structure consisting of the shortest-wavelength PL peak at 568 nm (2.18 eV), which has been conventionally assigned in literature to the 0–0 singlet excitonic transition, followed by a vibronic progression of about 0.16 eV [16]. The latter has been interpreted [15, 16] as a signature of exciton origin of the emission and indicates a coupling of the inter-ring carbon-carbon stretch vibrational mode at 1290 cm$^{-1}$ to the electronic transition.

A remarkable observation of this study is that the temperature dependent PL spectra of the above-described "islands" and "whiskers" structures differ drastically at higher temperatures, and their PL emission intensities exhibit very different temperature quenching behaviors. Let us first consider the rubrene "islands" samples. Firstly, the PL spectrum profile of the "islands" remains almost unchanged upon increasing temperature (Fig. 2, *a*), yet it demonstrates a notable blue shift with increasing temperature, which is more pronounced for the 0–1 transition at 614 nm (2.02 eV) as compared to the 0–0, most probably owing to the lack of self-absorption at longer wavelengths. A similar blue shift is quite typical for temperature-dependent PL spectra of disordered organic solids like vapor-deposited molecular glasses or semiconducting polymer films [17–19]. Secondly, the total PL intensity of the "islands" films shows an unusually small decrease (<15%) with increasing temperature from 5 K to room temperature (Fig. 2, *a*) as compared to rubrene solids, which implies a weak temperature quenching effect in these films. Such a behavior is in sharp contrast to temperature-dependent PL of rubrene single crystals, where a strong decrease of the total PL intensity by at least three orders of magnitude is typically observed as the temperature increases to room temperature [15]. Note that no additional PL bands are observed in the temperature-dependent PL spectra of this sample (Fig. 2, *a*).

The temperature-dependent PL spectra from matrix-isolated rubrene molecules dispersed in a neutral polystyrene host were also measured for comparison. The results are shown in the inset in Fig. 2, *a*. Similar spectra have been reported before for rubrene in a dilute solution [20, 21] which features an almost 100% fluorescence quantum yield. The inset in Fig. 2, *a* demonstrates that the temperature quenching of PL is *not* an inherent molecular property of this compound as the PL intensity of the matrix-isolated molecules manifests even a slight enhancement with increasing temperature from 5 to 160 K.

Fig. 2, *b* presents temperature-dependent PL spectra of the rubrene “whiskers” structures, which exhibit a very different and more complex behavior. First, the total PL emission from this sample manifests a strong decrease by more than 2 orders of magnitude (Fig. 2, *b*) with increasing temperature from 5 to 290 K (PL spectra at 200 and 290 K in Fig. 2, *b* are multiplied by a factor of 15). This behavior is quite in contrast to the PL of the “islands” sample and also to the molecular PL emission of rubrene dispersed in a polystyrene host film (cf. inset in Fig. 2, *a*). This implies a very efficient exciton quenching occurring in the “whiskers” structures, which is basically similar to that conventionally observed before in rubrene bulk single crystals. Second, the spectra profile of this sample changes considerably with temperature and an additional low-energy emission band emerges in the PL spectra at higher temperatures (Fig. 2, *b*). The PL spectrum becomes notably broader at $T \geq 200$ K and a new broad band peaking at 585 nm (2.11 eV) clearly dominates the room temperature emission spectrum.

Figures 3, *a* and 3b show normalized time-resolved PL spectra of the “islands” and “whiskers” structures, respectively, measured at a $T = 5$ K with different delay times $t_{\mathrm{del}} = 1$, 10, and 20 ns after the excitation. The prompt fluorescence spectrum was measured at the leading edge of the laser pulse excitation, so the delay time $t_{\mathrm{del}} = 1$ ns implies that the prompt fluorescence component was measured during the laser excitation pulse. The PL spectra of the “whiskers” structures manifested a clear red shift by about 10 nm upon increasing the delay time (Fig. 3, *b*); the same red shift was observed for the 0–1 peak at ∼615 nm. This observation implies an exciton transfer to low-lying states below the 0–0 transition in the course of exciton migration, and thus suggesting the presence of shallow bandgap states due to energetic disorder. The estimated lifetime of the emission component in the range 565–610 nm is about 8 ns at 5 K, which agrees with the value published for rubrene single crystals [22]. The red shift of the PL spectra with increasing delay time was found to be much less pronounced in the “islands” sample (Fig. 3, *a*), suggesting a less efficient exciton transfer to the low-lying states.

For comparison purposes, we have also measured PL spectra of the pristine rubrene powder that was used as source material for HWE growth of the rubrene films. Fig. 4, *a* shows temperature-dependent PL spectra of the rubrene powder at several selected temperatures, namely 5, 75, 100, 150, and 290 K. As one can see from Fig. 4, *a*, PL spectra of the powder change considerably from a well-resolved structure at 5 K to a broad unstructured band, peaking at 605 nm (2.05 eV) with increasing temperature and the PL intensity drops by about 2 orders of magnitude at $T = 290$ K. A similar effect was reported for rubrene single crystals [15] for which the room-temperature PL spectrum was also dominated by the broad band at 605 nm. Note that this is at variance with the data presented in Fig. 2, *b*; namely, the room-temperature PL spectra of the “whiskers” sample show a broad band peaking at 585 nm suggesting a different emitting species in these rubrene structures.

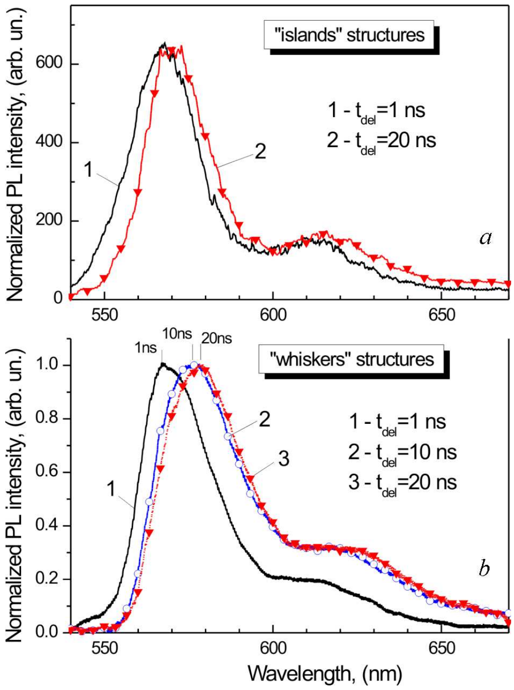

***Fig. 3.*** Normalized time-resolved PL spectra of the rubrene films at $T = 5$ K: “islands” (*a*) and “whiskers” (*b*) structures measured at different delay time $t_{\mathrm{del}} = 1$, 10, and 20 ns after the excitation (see text for details)

To clarify the role of oxidation and oxygen-related states, the same rubrene powder sample was oxidized by annealing in air at 100 °C for 14 h prior to the measurements that, is similar to the procedure described for thermal oxidation of rubrene single crystals [15]. Fig. 4, *b* depicts PL spectra of oxidized rubrene powder monitored under the same temper-

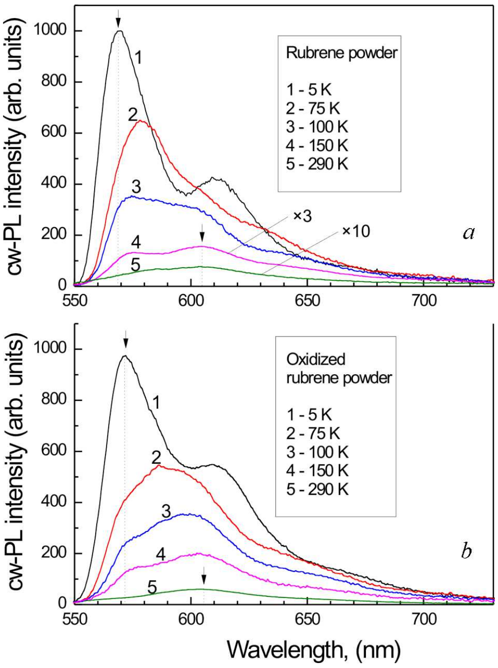

***Fig. 4.*** cw-PL spectra of pristine rubrene powder (*a*), and thermally oxidized powder (*b*) measured at different temperatures

atures as in Fig. 4, *a*. Comparison of Fig. 4, *a* and Fig. 4, *b* evidences that the 605 nm band relatively enhances in the oxidized sample (note that PL spectrum at 290 K in Fig. 4, *a* was multiplied by 10). No new PL band appears after such an oxidation, which gives us a reason to believe that the 605 nm band most probably originates from an oxygen-related emitting species.

### *3.3. Thermally stimulated luminescence*

To gain a deeper insight into the nature of defect states in the HWE-grown rubrene films we performed TSL studies to find out what dominates the charge-carrier trapping in these films. Fig. 5, *a* presents TSL glow curves after excitation with 366 nm light at 4.2 K of the same "islands" and "whiskers" structures (curves *1* and *2*, respectively) discussed above with respect to their PL properties. The different TSL intensity in these samples is most probably due to their different film thicknesses, as commonly observed before for other films of organic semiconductors. As evident from Fig. 5, *a*, all studied samples show a TSL signal at very low temperatures where at least two peaks at ∼20 and ∼40 K followed by a long tail lasting to 150 K can be distinguished and they are representative of very shallow charge trapping. The results obtained from rubrene "whiskers" structures clearly show an additional TSL band at ∼110 K, which is absent in "islands" films (Fig. 5, *a*), and it is significant for moderately deep charge-carrier traps created in "whiskers" films. An estimation of the activation energy at the TSL peak maximum at 110 K by means of fractional TSL yields a mean activation energy of 0.23 eV.

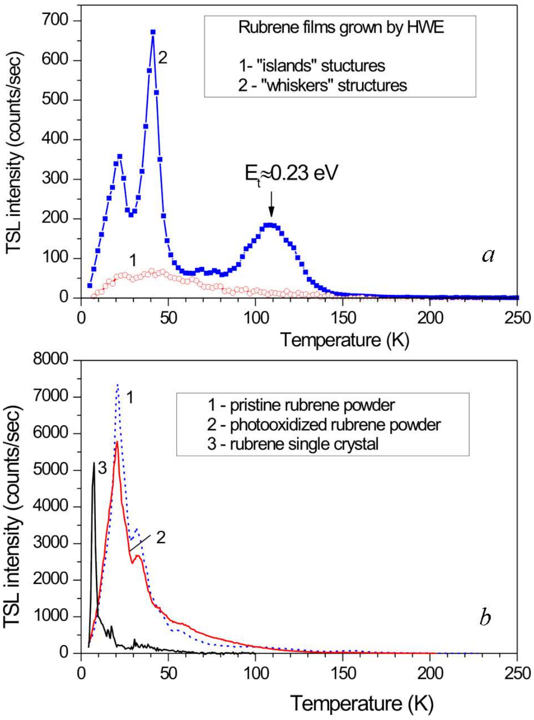

***Fig. 5.*** TSL glow curves of rubrene "islands" and "whiskers" layers at excitation with 365 nm light at 4.2 K (curve *1* and *2*, respectively) (*a*). TSL glow curve of the pristine rubrene powder (curve *1*), the same powder sample after preirradiation with a Hg lamp at room temperature for 7 h in air to induce photooxidation of rubrene (curve *2*), and a bulk rubrene single crystal (curve *3*) (*b*). TSL was excited with 365 nm light at 4.2 K

Fig. 5, *b* shows TSL spectra of rubrene powder. As one can see from curve 1 in Fig. 5, *b*, pristine powder features TSL peaks just at low temperatures (an intensive maximum at ∼20 K and a weaker one at 32 K) followed by a long broad tail lasting to ∼130 K. No apparent additional trap at 110 K is found in rubrene powder. Fig. 5, *b* shows also a TSL curve of a rubrene single crystal (curve *3*) which was measured under the same conditions and remarkably only a low-temperature TSL peak with maximum at 10 K was found, while no TSL signal was detected at higher temperatures. Such low-temperature TSL is a very rare phenomenon for molecular crystals. In order to check whether a moderately deep trap as found in “whiskers” structures can be created upon photooxidation of rubrene in air, we preirradiated the same powder sample for 7 h in ambient atmosphere at room temperature and after that measured the TSL. This photooxidation procedure was exactly the same as that described in the relevant study of oxygen-related defects in rubrene single crystals performed using the space-charge-limited-current (SCLC) technique [23]. The TSL result is depicted by curve *2* in Fig. 5, *b* and shows virtually no appreciable generation of a TSL band at 110 K and the obtained curves are within the reproducibility limit for the rubrene powder. Moreover, we have verified that a similar photooxidation of the “whiskers” structures did not result in any relative enhancement of the TSL peak at 110 K.

## 4. Discussion

The results presented above show that PL and TSL spectra of rubrene films grown by HWE are quite sensitive to the film morphology. Let us consider first the difference in temperature-dependent PL spectra of the “islands” and “whiskers” structures. As one can see from Fig. 2, these samples show a drastic difference with respect to the *temperature quenching effect* of the total PL intensity. The comparison with temperature-dependent PL of matrix-isolated rubrene molecules dispersed in an optically neutral polystyrene film clearly proves that the strong temperature quenching of the PL results from extrinsic quenching centers which can be reached by excitons in the course of their diffusion. As soon as the exciton diffusion is precluded in matrix-isolated molecules, no PL quenching was observed for rubrene diluted in a polystyrene film (inset in Fig. 2, *a*). The observed very weak temperature quenching in “islands” rubrene structures implies that exciton diffusion is limited in such samples most probably due to a rather disordered nature of such films. It is well known that diffusion processes could be strongly restricted in random lattices [24], therefore the exciton diffusion length greatly decreases with increasing disorder. On the other hand, “whiskers” structures showed a strong temperature PL quenching (orders of magnitude) basically similar to that observed for bulk rubrene single crystals [15]. This could imply a very different degree of crystalline order in “islands” and “whiskers” structures, which indeed has been confirmed by x-ray diffraction studies of such samples [25] – intensive Bragg peaks are found only in the latter type of films while no significant diffraction peaks is observed in the former ones. Thus, the probability for an exciton to reach some quenching center becomes small enough in disordered “islands’ structures. The situation is opposite in the rubrene “whiskers” samples for which crystallographic properties have been demonstrated by x-ray diffraction [25], so the exciton diffusion is facilitated in them. Thus, we conclude that different exciton diffusion in “islands” and “whiskers” structures is primary responsible for the different temperature quenching effect in these samples. A somewhat similar phenomenon is well known for triplet exciton emission in organic films, namely temperature-quenching of phosphorescence drastically reduces upon going from bulk material to diluted solid solutions.

Nevertheless, excitons are still mobile inside “islands” structures even at low temperature as evidenced by the observed blue shift in the PL transition energies with increasing temperature (Fig. 2, *a*). As already mentioned, disordered organic solids normally show a blue shift of their PL spectra with increasing temperature. Such a phenomenon has been thoroughly studied both experimentally and theoretically [17, 18] in different disordered organic materials and explained in terms of temperature-dependent dynamics of energetic relaxation of excitons within a Gaussian shaped density-of-states (DOS) distribution. It is considered that photogenerated excitons migrate to lower energy states via cascading downward hopping. This process is well documented by the observation of the so-called “spectral diffusion” effect in transient PL studies of disordered organic solids and it can also be seen for rubrene films in Fig. 3. The larger spectral diffusion observed in “whiskers” structures (Fig. 3, *b*) as compared to “islands” (Fig. 3, *a*) agrees with the notion of stronger exciton diffusion in the “whiskers”. The energetic relaxation of excitons towards tail states of the DOS can be effectively compensated by thermal activation, allowing excitons to reach dynamic equilibrium with the lattice. Increasing temperature results in raising the dynamic equilibrium energy of the exciton population, thus explaining the blue shift of the PL spectra, since the excitons tend to settle at energetically higher localized states. In other words, the observed blue shift of the PL peaks in "islands" structures reflects the thermally activated population of higher energy localized states and testifies to the presence of some amount of energetic disorder in these materials. On the other hand, the presence of energetic disorder in this film is proved by the observation of a low-temperature band in TSL spectra (Fig. 5, *a*, curve *1*) which is typically originates from a shallow charge-carrier trapping on the tail states of the intrinsic DOS distribution (for detailed explanations see Refs. [11–14]).

Let us further discuss a possible origin of additional PL bands observed in PL spectra of rubrene "whiskers" structures, originated from a specific charge carriers trap (centered at $E_t = 0.23$ eV) created in such films. In contrast to the "islands", both the rubrene "whiskers" structures and the rubrene powder clearly show additional band gap centers in PL emission, which becomes pronounced at higher temperatures. This unambiguously implies the presence of defect states in these materials, which can capture excitons at sufficiently high temperature since the exciton diffusion is a thermally activated process and enhances with temperature. The defects also give rise to the above mentioned PL quenching effect as they normally are purely emitting species.

The defects in organic materials can be classified [26, 27] as of chemical [28] (due to presence of incidental impurities or oxidative defects) or of structural/morphological origin. Structural defects, which are especially important in chemically perfect materials [27, 29], can result from specific molecular configurations/arrangements where the intermolecular interaction is locally increased, thus traps for both neutral excitons and charge carriers are created [26, 27]. It was well documented that structure defects in molecular crystals could be due to dislocations, grain boundaries, *etc.* [26, 27]. They produce band gap states observed in PL [27,30] and by charge trapping spectroscopy for charge carriers [27].

The room temperature PL spectrum of the "whiskers" is dominated by the broad structureless band peaking at 585 nm (2.11 eV), which is shifted by 0.07 eV below the observed 0–0 exciton transition band at 568 nm (2.18 eV) (Fig. 2, *a*). A band gap transition dominates also the room-temperature PL spectrum of rubrene powder as well (Fig. 4, *a*); however, the corresponding additional PL band is somewhat different – it is located at 605 nm. It was already shown that the same 605 nm band dominates the room temperature PL of the high-purity rubrene single crystals [15]. This implies that different defect states are dominant in the "whiskers" structures and rubrene powder (single crystal). The fact that the 605 nm band is relatively enhanced upon oxidation of the rubrene powder (Fig. 4, *b*) allows to conclude, that this band is likely due to an oxygen-related state. No enhancement of the 585 nm band was found in oxidized samples, so we assign it to intrinsic defects, most probably of structural origin which is specific for HWE-grown rubrene films of "whisker-like" morphology.

The PL data correlate well with TSL results presented in Fig. 5, *a*, which clearly show a specific moderately deep ($E_t = 0.23$ eV) charge-carrier trap created in "whiskers" structures. As mentioned in the preceding section, TSL of studied samples shows two different kinds of signals:

(i) A low-temperature signal featuring two closely situated peaks at ∼20 and ∼40 K, followed by a long tail to higher temperatures, which is observed in all studied samples and is inherent to rubrene thin films (Fig. 5). It shows all characteristic fingerprints of the tail DOS states typically observed in disordered organic semiconductor films and demonstrates that the tail DOS states can act as shallow traps at very low temperatures [10–13]. This conclusion perfectly agrees with temperature-dependent space-charge-limited-current (TD-SCLC) spectroscopy results [23] for rubrene single crystals, revealing the existence of an exponentially varying shallow trap density within ∼0.1 eV from the band edge, reminiscent of band tails. Interestingly, for rubrene single crystals we found a TSL peak at an even lower temperature (∼10 K), that is probably the lowest-temperature TSL band ever observed for molecular crystals and this phenomenon requires further investigation. It is worth mentioning that a pronounced peak at ∼10 K in a low-temperature thermal conductivity scan has been reported for rubrene crystals [31], which was taken as evidence for an extremely low-level defect density in such crystals.

(ii) The TSL band at 110 K, which is only observed in rubrene "whiskers" structures, is not observed in rubrene powder, thus suggesting that it is not due to an accidental impurity in rubrene material, but rather is structure-related. The 110 K TSL band cannot be due to oxygen-related defects, as it is not generated upon deliberate photooxidation of the rubrene powder and crystals. It is worth noting that a distinct hole bulk trap at 0.27 eV above the valence band was reported for rubrene single crystals by TD-SCLC study [23]. Considering the very similar trap depth found in our TSL studies of rubrene "whiskers", and the fact that rubrene is a p-type organic semiconductor, we assign the TSL peak at 110 K to a hole trap. However, in contrast to Ref. [23], we did not observe the generation of this hole trap in rubrene films or crystals after a similar photooxidation procedure as that done in Ref. [23]. This seems not to be surprising because oxygen-related moieties typically possess electron acceptor properties and are thus expected to trap electrons rather than holes. Besides, a strong sensitivity of this trap at 110 K (Fig. 5) to the structure of rubrene solids strongly suggests that the hole trap is due to a structure-related defect.

Finally, we show that the additional PL band at 585 nm and the TSL peak at 110 K are most probably a manifestation of the same structural defect. This is supported by the following:

(i) This defect appears in PL and TSL spectra of the same samples ("whiskers"), whereas both the 585 nm PL band and TSL peak at 110 K are absent in other rubrene films and rubrene powder/single crystals. (ii) It is well known that such a defect is of structural origin and should create a trap for both excitons and charge carriers due to enhanced electronic polarization at such a defect state. Previous theoretical calculations [26, 27] showed that the trap for charge carriers should be approximately 3 times deeper than the exciton trap associated with the same structural defect [26]. This indeed seems to be the case for HWE-grown "whiskers" structures where the charge trap is of 0.23 eV depth, and the exciton trap is shifted by 0.07 eV shifted with respect to the 0–0 exciton transition.

## 5. Conclusion

We found that rubrene HWE-grown films of "whisker-like" morphology show a distinct defect state of structure-related origin, creating both a trap for singlet excitons (PL band at 585 nm) and a moderately deep trap ($E_t = 0.23$ eV) for holes responsible for the TSL peak at 110 K. This defect state is pronounced specifically in HWE-grown "whiskers" structures and is not observed in rubrene films of "islands-like" morphology or pristine rubrene powder/crystals. The latter rubrene samples feature just low-temperature TSL peaks around 30 K, implying the existence of a distribution of shallow localized states, reminiscent of band tails, resulting from intrinsic disorder in the samples. Besides, we found an amazing very shallow charge carrier trapping in rubrene single crystals giving rise to a TSL peak at ∼10 K. Temperature-dependent PL spectra of rubrene films grown by HWE are found to depend substantially on the morphology of the rubrene films. The intrinsic exciton emission dominates the PL spectra of the "islands" structures at all temperatures used for measurements accompanied by only weak temperature-induced PL quenching. PL spectra of "whiskers" structures change considerably with temperature, clearly reveling additional bandgap emission states at higher temperatures and their PL intensity is quenched by several orders of magnitude with increasing temperature. This effect was attributed to very different exciton diffusivities in the two types of samples, governed by their different crystalline order.

1. V. Podzorov, E. Menard, A. Borissov, V. Kiryukhin, J.A. Rogers, M.E. Gershenson. Intrinsic charge transport on the surface of organic semiconductors. *Phys. Rev. Lett.* **93**, 086602 (2004).
2. M. Yamagishi, J. Takeya, Y. Tominari, Y. Nakazawa. High-mobility double-gate organic single-crystal transistors with organic crystal gate insulators. *Appl. Phys. Lett.* **90**, 182117 (2007).
3. J. Takeya, J. Kato, K. Hara, M. Yamagishi, R. Hirahara, K. Yamada, Y. Nakazawa, S. Ikehata, K. Tsukagoshi, Y. Aoyagi, T. Takenobu, Y. Iwasa. In-crystal and surface charge transport of electric-field-induced carriers in organic single-crystal semiconductors. *Phys. Rev. Lett.* **98**, 196804 (2007).
4. Se-W. Park, S.H. Jeong, J.-M. Choi, J.M. Hwang, J.H. Kim, S. Im. Rubrene polycrystalline transistor channel achieved through in situ vacuum annealing. *Appl. Phys. Lett.* **91**, 033506 (2007).
5. M. Nothaft, J. Pflaum. Thermally and seed-layer induced crystallization in rubrene thin films. *Phys. Status Solidi B* **245**, 788 (2008).
6. C.H. Hsu, J. Deng, C.R. Staddon, P.H. Beton. Growth front nucleation of rubrene thin films for high mobility organic transistors. *Appl. Phys. Lett.* **91**, 193505 (2007).
7. T. Nguyen, T.N. Manh, H. Sitter, D. Stifter. Preparation of pristine and Ba-doped $C_{60}$ films by hot-wall epitaxy. *J. Cryst. Growth* **174**, 828 (1997).

8. A. Andreev, G. Matt, C.J. Brabec, H. Sitter, D. Badt, H. Seyringer, N.S. Sariciftci. Highly anisotropically self-assembled structures of para-sexiphenyl grown by hot-wall epitaxy. *Adv. Mater.* **12**, 629 (2000).
9. H. Sitter. Silicon Forever! Really?. In: *Organic Nanostructures for Next Generation Devices.* Edited by K. Al-Shamery, H.-G. Rubahn, H. Sitter (Springer-Verlag, 2008), p. 327–334.
10. A. Kadashchuk, A. Andreev, H. Sitter, N.S. Sariciftci, Y. Skryshevski, Y. Piryatinski, I. Blonsky, D. Meissner. Aggregate states and energetic disorder in highly ordered nanostructures of para-sexiphenyl grown by hot wall epitaxy. *Adv. Funct. Mater.* **14**, 970 (2004).
11. A. Kadashchuk, D.S. Weiss, P.M. Borsenberger, S. Nešpùrek, N. Ostapenko, V. Zaika. The origin of thermally stimulated luminescence in neat and molecularly doped charge transport polymer systems. *Chem. Phys.* **247**, 307 (1999).
12. A. Kadashchuk, Yu. Skryshevski, Yu. Piryatinski, A. Vakhnin, E.V. Emelianova, V.I. Arkhipov, H. Bässler, J. Shinar. Thermally stimulated photoluminescence in poly(2,5-dioctoxy p-phenylene vinylene). *J. Appl. Phys.* **91**, 5016 (2002).
13. A. Kadashchuk, Yu. Skryshevski, A. Vaknin, N. Ostapenko, E.V. Emelianova, V.I. Arkhipov, H. Bassler. Thermally stimulated photoluminescence in disordered organic materials. *Phys. Rev. B* **63**, 115205 (2001).
14. V.I. Arkhipov, E.V. Emelianova, A. Kadashchuk, H. Bässler. Hopping model of thermally stimulated photoluminescence in disordered organic materials. *Chem. Phys.* **266**, 97 (2001).
15. O. Mitrofanov, D.V. Lang, C. Kloc, J.M. Wikberg, T. Siegrist, W.-Y. So, M.A. Sergent, A.P. Ramirez. Oxygen-related band gap state in single crystal rubrene. *Phys. Rev. Lett.* **97**, 166601 (2006).
16. M. Kytka, L. Gisslen, A. Gerlach, U. Heinemeyer, J. Kovač, R. Scholz, F. Schreiber. Optical spectra obtained from amorphous films of rubrene: Evidence for predominance of twisted isomer. *J. Chem. Phys.* **130**, 214507 (2009).
17. H. Bässler. Exciton and charge carrier transport in random organic solids. In: *Disordered Effect on Relaxational Processes* (Springer-Verlag, 1994).
18. H. Bässler, B. Schweitzer. Site-selective fluorescence spectroscopy of conjugated polymers and oligomers. *Acc. Chem. Res.* **32**, 173 (1999).
19. S. Guha, J.D. Rice, Y.T. Yau, C.M. Martin, M. Chandrasekhar, H.R. Chandrasekhar, R. Guentner, P. Scanduicci de Freitas, U. Scherf. Temperature-dependent photoluminescence of organic semiconductors with varying backbone conformation. *Phys. Rev. B* **67**, 125204 (2003).
20. W.A. Yee, V.A. Kuzmin, D.S. Kliger, G.S. Hammond, A.J. Twarowshi. Charge carrier trapping effect by luminescent dopant molecules in single-layer organic light emitting diodes. *J. Am. Chem. Soc.* **79**, 5104 (1979).
21. M. Uchida, C. Adachi, T. Koyama, Y. Taniguchi. Charge carrier trapping effect by luminescent dopant molecules in single-layer organic light emitting diodes. *J. Appl. Phys.* **86**, 1680 (1999).
22. S.J. Strickler, R.A. Berg. Relationship between absorption intensity and fluorescence lifetime of molecules. *J. Chem. Phys.* **37**, 814 (1962).
23. C. Krellner, S. Haas, C. Goldmann, K.P. Pernstich, D.J. Gundlach, B. Batlogg. Density of bulk trap states in organic semiconductor crystals: Discrete levels induced by oxygen in rubrene. *Phys. Rev. B* **75**, 245115 (2007).
24. P.W. Anderson. Absence of diffusion in certain random lattices. *Phys. Rev.* **109**, 1492 (1958).
25. T. Djuric, H.-G. Flesch, M. Koini, Sh.M. Abd Al-Baqi, H. Sitter, R. Resel. Structural properties of rubrene thin films grown on mica. In: *Interface Controlled Organic Thin Films.* Edited by H.-G. Rubahn, H. Sitter, G. Horowitz, K. Al-Shamery (Springer, 2009), p. 49–52.
26. E.A. Silinsh. *Organic Molecular Crystals. Their Electronic States* (Springer, 1980).
27. M. Pope, C. E. Swenberg. *Electronic Processes in Organic Crystals and Polymers* (Oxford University Press, 1999).
28. K.H. Probst, N. Karl. Energy levels of electron and hole traps in the band gap of doped anthracene crystals. *Phys. Status Solidi A* **27**, 499 (1975).
29. H. Sirringhaus, P.J. Brown, R.H. Friend, M.M. Nielsen, K. Bechgaard, B.M.W. Langeveld-Voss, A.J.H. Spiering, R.A.J. Janssen, E.W. Meijer, P. Herwig, D.M. de Leeuw. Two-dimensional charge transport in self-organized, high-mobility conjugated polymers. *Nature* **401**, 685 (1999).
30. V.A. Lisovenko, M.T. Shpak, B.G. Antonjuk. Edge dislocations – emission centres in deformed anthracene single crystals. *Chem. Phys. Lett.* **42**, 339 (1976).
31. Y. Okada, M. Uno, J. Takeya. Low-temperature thermal conductivity of rubrene single crystals: quantitative estimation of defect density in bulk and film crystals. *MRS Proceedings* **1154**, B10-59 (2009).

Received 30.12.25

*Ю. Скришевський, О. Вахнін,*
*Ю. Пирятинський, Шайма Абд Аль-Бакі,*
*Г. Зіттер, А. Кадащук*

## МОРФОЛОГІЧНО-ЗАЛЕЖНІ СТАНИ ДЕФЕКТІВ У КРИСТАЛІЧНИХ ПЛІВКАХ РУБРЕНУ, ВИРОЩЕНИХ МЕТОДОМ ЕПІТАКСІЇ З ГАРЯЧИМИ СТІНКАМИ

Наноструктури рубрену, вирощені методом епітаксії з гарячими стінками на підкладинках зі слюди, досліджено за допомогою фотолюмінесцентної (ФЛ) спектроскопії та методом термостимульованої люмінесценції (ТСЛ). Різні морфології плівок, що були охарактеризовані методами оптичної й електронної мікроскопії, отримували шляхом варіювання умов осадження. Встановлено, що температурно-залежні ФЛ спектри істотно залежать від морфології шарів рубрену. Плівки, вирощені протягом короткого часу осадження, демонструють ФЛ спектри, в яких домінує випромінювання власних екситонів, зі слабким загасанням інтенсивності сигналу в умовах зростання температури. Натомість плівки, вирощені протягом довших часів осадження і в умовах вищих температур підкладинки, виявляють додаткові випромінювальні стани, а їх інтенсивність ФЛ зазнає сильного температурного гасіння. Основними є такі результати цієї роботи: (i) у плівках рубрену, вирощених за умов тривалого часу осадження і підвищеної температури підкладинки, формується специфічний структурно-зумовлений дефектний стан, який діє як окрема пастка для дірок з глибиною 0,23 еВ, що визначено методом ТСЛ; цей дефект зумовлює появу широкої низькоенергетичної смуги випромінювання, що домінує в спектрах ФЛ за кімнатної температури; (ii) контрольоване окиснення кристалів рубрену демонструє, що пастка для дірок, виявлена методом ТСЛ, не пов'язана з киснем, а має походження від власного кристалічного дефекту; (iii) метод ТСЛ виявляє неперервний розподіл мілких локалізованих станів, подібний до хвостів зон, які виникають внаслідок власного енергетичного розупорядкування в матеріалі. Ці мілкі стани відповідають за низькотемпературні смуги ТСЛ поблизу температури 30 К і за зсув спектрів ФЛ у довгохвильовий бік спектра зі збільшенням часу затримки, яке спостерігається в часороздільних вимірюваннях ФЛ.

*Ключові слова*: рубрен, епітаксія з гарячими стінками, наноструктури, дефектний стан, морфологія плівки, енергетичне розупорядкування, термічно стимульована люмінесценція.